URSI GASS 2021, Rome, Italy, 28 August - 4 September 2021

HF Pulsed Thundercloud Emission Observed in the Upper Volga Region of Russia

Anatoly N. Karashtin*[(1)(2)] Yury V. Shlyugaev[(1)], and Olga S. Karashtina[(2)]
(1) Institute of Applied Physics, Russian Academy of Sciences, Nizhny Novgorod, Russian Federation
(2) Radiophysical Research Institute, Nizhny Novgorod State University, Nizhny Novgorod, Russian Federation

Abstract

Radio frequency emission from thunderclouds is analysed on the base of measurements over a wide frequency range with a high temporal resolution. This emission mainly consists of short sub-microsecond bi-polar pulses. Characteristics of the pulses are studied at different stages of lightning discharge development as well as for events does not leading to lightning.

1 Introduction

Observations of radio emission from lightning discharges in a wide frequency range from 50 kHz to 30 MHz covering long, medium and short waves with a high temporal resolution are first described in [1, 2]. In these works it was found that the radio emission of lightning begins suddenly with a sequence of bipolar sub-microsecond pulses. Further research showed that at the stages of preliminary preparation, initiation and development of lightning, up to a return stroke, radio emission in the specified frequency range consists of a large number of such pulses [3]. The presence of submicrosecond bipolar pulses in lightning radio emission was also reported in [4]. Broadband recording of radio emission from lightning discharges with a high temporal resolution was also performed in [5, 6], where the general behavior of the recorded radio emission is similar to that of [1, 2, 3], but the presence of submicrosecond bipolar pulses was not clearly distinguished. Relatively recently measurements of radio emission from lightning with nanosecond time resolution were carried out with the LOw-Frequency ARray (LOFAR) [7] radio telescope operating in the frequency range 10–90 MHz.

2 Instrumentation

Observations were carried out using a setup for recording the waveform of short sub-microsecond electromagnetic pulses. The installation was placed at the receiving point in the Nizhny Novgorod region (geographical coordinates 56.15N, 44.32E). It consists of four antenna modules similar to described in [1, 2] spaced by about 300 m in the east–west direction and about 75 m in the south–north one. Each antenna module contains three antennas: vertical electric dipole to measure the vertical component of the electric field and two crossed loops to measure mutually orthogonal horizontal components of the magnetic field. Amplifiers serve to match antennas to the cables connected antenna modules to data logging systems providing frequency range from 50 kHz to 30 MHz. All the cables are of the same length of about 60 m. Two data logging systems are used for pairs of antenna modules spaced in the east–west direction. Data recording systems use four-channel 14-bit analog-to-digital converters (ADCs) with a maximum clock frequency of 60 MHz and an internal memory of 1 GB. They record the radio emission received by the antenna modules continuously into a circular buffer organized in the internal memory of the ADC. At the moment of a lightning discharge a trigger pulse is generated by a special device that receive low-frequency (below 10 kHz) radio emission accompanying the lightning discharge to start wideband registration. The trigger device is located nearby one of the data logging systems. The second data logging system gets a trigger pulse via a fiber-optic cable, time delay in the cable was accurately measured. After the arrival of the trigger pulse data recording continues for some predetermined time, after which the entire buffer was rewritten onto the hard drive. The use of a common trigger pulse guarantees the recording of the same lightning by both data logging systems. The ADC clock frequency of 60 MHz and the recording duration of each event of 1.5 seconds with a pre-history of 0.5 seconds was choosen in the observations. Due to the high level of interference in the low-frequency part of the receiving band in the electric field channel, only magnetic (loop) antennas were used in the observations. The installation operated continuously in patrol mode and recorded the radio emission of lightning that took place in its immediate vicinity. Additionally, one of the loop antennas was connected to the separate data logger that allowed to record single channel data with 50 MHz tact frequency quasi-continuously for several hours with a loss of approximately 3–5% of the data.

3 Observations

A large number of events was recorded during several thunderstorms occured near the receiving point. Most of them correspond to lightning discharges. An example of such event registered at about 15:04 UT on May 15, 2019 is presented in Figure 1. Amplitude of the radio emission is shown in the upper panel of the Figure. The event starts suddenly with rare bi-polar submicrosecond pulses of a rather large amplitude. A sequence of such pulses that in this particular case lasted for about 200 milliseconds. This period can be considered as a pre-conditioning stage of the lightning discharge. For other events this stage could lasted from few to several hundreds of millisecond. For the analysis we used events with rather long pre-conditioning stage to have enough number of pulses for statistics. The root mean square (RMS) of the emission calculated at 100 microsecond intervals is shown in the middle panel of the Figure. RMS has moderate values with strong fluctuations at the pre-conditioning stage. Next, at about 40 milliseconds before trigger fluctuations become much weaker thet can be interpreted as the beginning of step leader stage of the lightning. The event ends at trigger time with a sharp increase of RMS that can be considered as return stroke. Kurtosis calculated at the same intervals can serve as an indicator of pulsed nature of the emission. It is shown in the bottom panel of the Figure, and has very high values at the pre-conditioning stage decreasing during the step leader stage to background value at return stroke. Its behavior confirms pulsed nature of emission at the pre-conditioning stage.

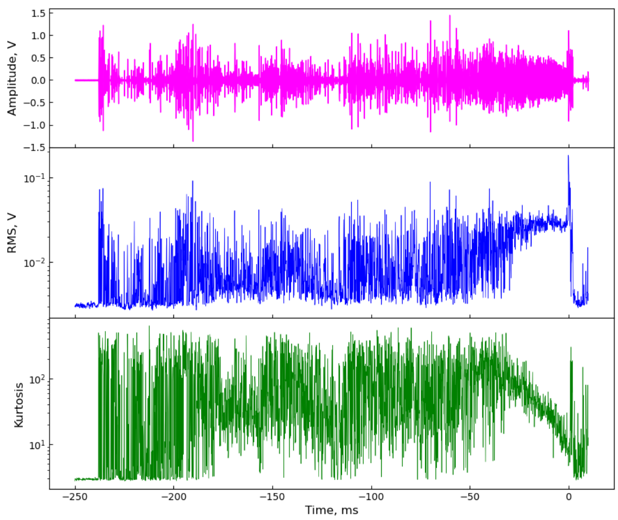

Figure 1. Radio frequency event registered at about 15:04 UT on May 15, 2019 thunderstorm. This event corresponds to a cloud-to-ground lightning. Top panel: Amplitude of the radio emission versus time. 1 V of the ADC output approximately corresponds to the electric field strength of 1 V/m. Middle panel: The root mean square values of the radio emission calculated on the time intervals of 100 microseconds. Bottom panel: Kurtosis of the radio emission calculated over the same time intervals. Time is given in milliseconds from the trigger.

Not in all events a pre-conditioning stage is followed by step leader and return stroke stages. An example is shown in Figure 2 for the event recorded at about 15:27 UT on May 22. This event also starts suddenly with rare bi-polar submicrosecond pulses of a rather large amplitude, but the kurtosis remains high during the whole event.

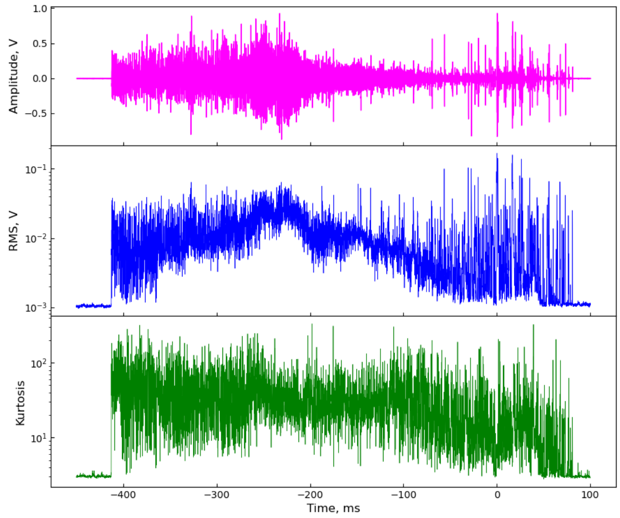

Figure 2. The same as in Figure 1 for the event registered at about 15:27 UT on May 22, 2019 thunderstorm. This event seems does not correspond to lightning. Time is given in milliseconds from the trigger.

4 Characteristics of pulsed radio emission

The main characteristics of pulsed radio emission are pulse count rate and amplitude distribution. Count rates calculated per millisecond are presented in Figures 3, 4. For the first event count rate was at approximately the same low level during the pre-conditioning stage. At the step leader stage it grew continuously by more than an order to the return stroke. For the second event there was some growing of count rate at about -250 ms, but then the count rate came back to the previous level.

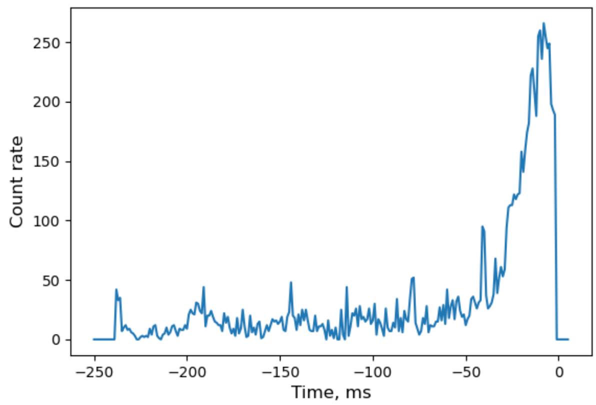

Figure 3. Count rate of pulses per millisecond in the radio frequency emission for the event presented in Figure 1. Time is given in milliseconds from the trigger.

Amplitude distibutions are shown in Figures 5, 6. For the first event one can see clear difference of distribution functions at the pre-conditioning and step leader stages, namely the absence of pulses with large amplitudes. For the second event distribution function remains the same for different

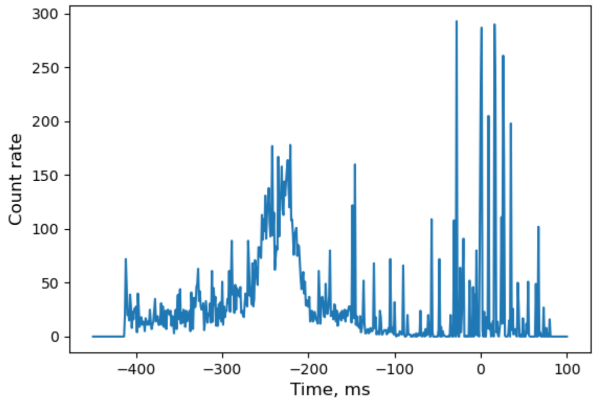

Figure 4. Count rate of pulses per millisecond in the radio frequency emission for the event presented in Figure 2. Time is given in milliseconds from the trigger.

parts of the record.

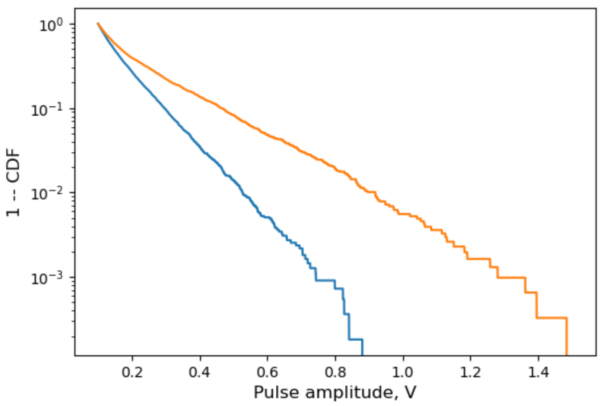

Figure 5. Complementary cumulative distribution function (1 – CDF) for the event presented in Figure 1. Blue line is for pre-conditioning stage, and red one for the step leader stage. Time is given in milliseconds from the trigger.

5 Conclusions

The suddenness of the onset of radio emission from a thundercloud, always with a pulse of high amplitude, and the fact that the shape, duration, and intensity of the observed pulses correspond to the theory of runaway breakdown during the passage of extensive air showers caused by high-energy cosmic rays through a region of intense electric field inside a thundercloud in the presence of hydrometeors [8], allow us to propose the following scenario for the generation of radio frequency emission in a thundercloud. When a region of a sufficiently strong electric field appears inside a thundercloud the passage of an EAS through this region gives seed energetic particles for the development of breakdown. The observed radio emission event is initiated by a particle of rather high energy that can be estimated as 10^{16} eV based on an intensity of the initial pulse. As a result of the combined action of EAS and runaway breakdown a significant number of free thermal electrons appears

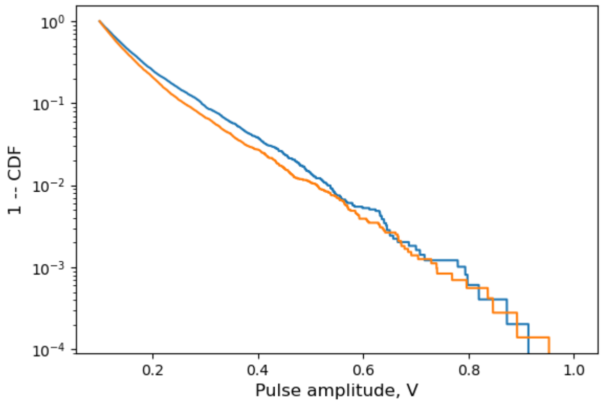

Figure 6. Complementary cumulative distribution function (1 – CDF) for the event presented in Figure 2. The vent was divided into two parts, blue and red lines are for them. Time is given in milliseconds from the trigger.

which quickly adhere to molecules and form a large number of ions. Later the process is supported by EAS caused by particles of substantially lower energies $\geq 10^{14}$ eV passing through the already ionized region of the thundercloud. A region of increased conductivity saturated with light ions is formed inside a thundercloud in such a way, and prerequisites are created for the collection of charge, the strengthening of the electric field, and the initiation of a lightning discharge, the development of which, however, may not occur.

6 Acknowledgements

This work was supported by the Russian Science Foundation through the grant #19-17-00183.

References

[1] A. V. Gurevich, L. M. Duncan, A. N. Karashtin, K. P. Zybin, “Radio emission of lightning initiation,” *Phys. Lett. A*,**312**, 3–4, June 2003, pp. 228–237, doi:10.1016/s0375-9601(03)00511-5.

[2] A. N. Karashtin, Y. V. Shlyugaev, A. V. Gurevich, “High-frequency radio emission of the lightning discharge,” *Radiophys. Quantum Electron.*, **48**, 9, September 2005, pp. 711–719, doi:10.1007/s11141-005-0115-5.

[3] A. V. Gurevich, A. N. Karashtin, “Radio emission structure of cloud-to-ground lightning discharge,” *Phys. Lett. A*, **375**, 7, February 2011, pp. 1128–1134, doi:10.1016/j.physleta.2010.12.053.

[4] A. Nag and V. A. Rakov, “Electric field pulse trains occurring prior to the first stroke in negative cloud-to-ground lightning,” *IEEE Trans. Electromagn. Compat.*, **51**, 1, February 2009, pp. 147–150, doi:10.1109/TEMC.2008.2005488.

[5] Y. Lan, Y. Zhang, W. Dong, W. Lu, H. Liu, D. Zheng, "Broadband analysis of chaotic pulse trains generated by negative cloud-to-ground lightning discharge," *J. Geophys. Res.*, **116**, D17, September 2011, D17109, doi:10.1029/2010JD015159.

[6] Y. Zhang, Y. Zhang, C. Li, W. Lu, D. Zheng, "Simultaneous optical and electrical observations of "chaotic" leaders preceding subsequent return strokes," *Atmos. Res.*, **170**, March 2016, pp. 131–139, doi:10.1016/j.atmosres.2015.11.012.

[7] B. M. Hare et al., "LOFAR lightning imaging: Mapping lightning with nanosecond precision,", *J. Geophys. Res. Atmos.*, **123**, March 2018, pp. 2861–2876, doi:10.1002/2017JD028132

[8] A. V. Gurevich, A. N. Karashtin, "Runaway breakdown and hydrometeors in lightning initiation," *Phys. Rev. Lett.*, **110**, 18, May 2013, 185005, doi:10.1103/physrevlett.110.185005.